

Controlling and reversing the quantum-to-classical transition of a quantum walk by driving the coin

Peng Xue¹ and Barry C. Sanders²

¹*Department of Physics, Southeast University, Nanjing 211189, China*

²*Institute for Quantum Information Science, University of Calgary, AB T2N 1N4, Canada*

(Dated: September 18, 2012)

We show that the standard quantum-walk quantum-to-classical transition, characterized by ballistic-to-diffusive spreading of the walker’s position, can be controlled by externally modulating the coin state. We illustrate by showing an oscillation between classical diffusive and quantum ballistic spreading using numerical and asymptotically exact closed-form solutions, and we prove that the walker is in a controllable incoherent mixture of classical and quantum walks with a reversible quantum-to-classical transition.

PACS numbers: 03.67.Mn, 03.65.Ta, 05.40.Fb, 03.67.Ac

The quantum walk on a lattice [1, 2] is an important branch of quantum information research for several reasons [3]. The quantum walk concept drives breakthroughs in quantum algorithms, including speeds up for quantum searches [4] and exponential speed-ups of graph traversal compared with the best known classical algorithms for such tasks [5, 6]. Beyond quantum algorithms and into the physical world, quantum walks are evident in spin-chain quantum transport [7] and photosynthetic excitonic energy transport [8]. Quantum walks serve as one model for quantum computation [9, 10] alongside other models such as circuit [11], measurement-based [12], adiabatic [13] and topological quantum computing [14]. Experimental realizations of quantum walks abound with successes having been reported in nuclear magnetic resonance [15], ion traps [16] and photons [17, 18].

Decoherence is especially important in quantum walk implementations, both because it deleteriously destroys unitarity with consequences such as transforming the ballistic spreading to diffusive spreading [19, 20] and because of the beneficial property of enabling tuning of quantum walk dynamics [21]. Typically decoherence is characterized by the rate of spreading of the walker’s position after tracing over the coin state, and ballistic spreading is ‘quantum’ and diffusive spreading is ‘classical’. Here we show that controlling the walker’s coin in an appropriate time-dependent way enables the walker to achieve diffusive spreading and later back to ballistic, i.e. transferring between classical and quantum behavior in a controlled way. Our result challenges the paradigm of the quantum-to-classical transition for a random walk and furthermore points to external coin manipulation as a means for controlling quantum walks.

The joint walker-coin state ρ_{wc} is a trace-class positive operator on the Hilbert space $\mathcal{H} = \mathcal{H}_w \otimes \mathcal{H}_c$ such that $\mathcal{H}_w = \text{span}\{|x\rangle; x \in \mathbb{Z}\}$ with $|x\rangle$ the orthonormal walker position states on a regular integer lattice, and $\mathcal{H}_c = \text{span}\{|\pm\rangle\}$ with $|\pm\rangle$ the two coin states. If the walker-coin system undergoes periodic unitary steps, the evolution

operator is given by

$$U := F(\mathbb{1} \otimes C), \quad C := H = \frac{1}{\sqrt{2}} \begin{pmatrix} 1 & 1 \\ 1 & -1 \end{pmatrix} \quad (1)$$

for $\mathbb{1}$ the identity, H the Hadamard operator and

$$F := S \otimes |+\rangle\langle+| + S^\dagger \otimes |- \rangle\langle-|, \quad S := \sum_x |x+1\rangle\langle x|. \quad (2)$$

The walker’s evolving state is

$$\rho_{wc}(t) = U^t \rho_{wc}(0) := (U^\dagger)^t \rho_{wc}(0) U^t \quad (3)$$

for discrete time parameter $t \in \mathbb{Z}$. The case of the driven coin is more complicated and is treated below.

We now generalize for the case of the driven coin. Prior to each unitary coin ‘flip’, a completely-positive trace-preserving map $\mathcal{E}(t, 0) : \rho_c(0) \mapsto \rho_c(t)$ is applied to the coin. The map can be decomposed into the operator sum

$$\mathcal{E}\rho_c = \sum_{n \in \{0, \pm\}} A_n \rho_c A_n^\dagger, \quad \sum_{n \in \{0, \pm\}} A_n^\dagger A_n = \mathbb{1} \quad (4)$$

with

$$A_0 = \sqrt{\kappa(t)}\mathbb{1}, \quad A_\pm = \sqrt{1 - \kappa(t)}\mathcal{P}^\pm, \quad \mathcal{P}^\pm = |\pm\rangle\langle\pm|, \quad (5)$$

corresponding to a coin with a probability $(1 - \kappa)$ of being measured at each step. If $\kappa(t) = e^{-\gamma t}$, this mapping is equivalent to a pure dephasing channel for γ a dephasing rate.

Although $\kappa(t)$ can be general, we choose to illustrate controllable, reversible quantum-to-classical walk transitions by employing oscillatory $\kappa(t) \equiv \cos \eta t$, which realizes the periodic dynamical map

$$\begin{aligned} \mathcal{E}\rho_c &= \kappa(t)\rho_c + [1 - \kappa(t)] [\mathcal{P}^+ \rho_c \mathcal{P}^+ + \mathcal{P}^- \rho_c \mathcal{P}^-], \\ \rho_c^{00} &\mapsto \rho_c^{00}, \quad \rho_c^{01} \mapsto \cos \eta t \rho_c^{01}, \quad \rho_c^{10} \mapsto \cos \eta t \rho_c^{10}, \quad \rho_c^{11} \mapsto \rho_c^{11}. \end{aligned} \quad (6)$$

The walker’s reduced state and resultant position distribution at time t are

$$\rho_w(t) = \text{Tr}_c \rho_{wc}(t), \quad P_w(x, t) = \langle x | \rho_w(t) | x \rangle \quad (7)$$

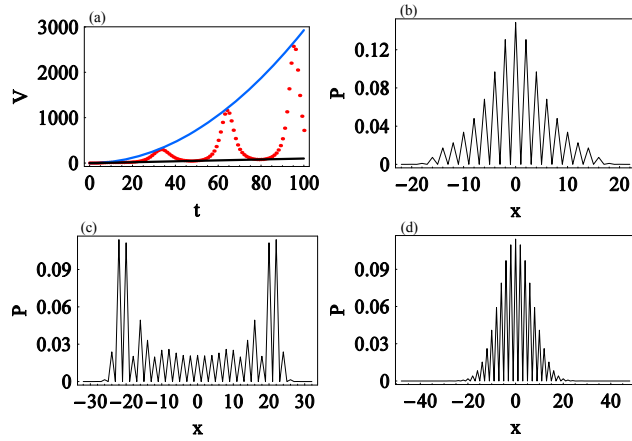


FIG. 1: (Color online) (a) Numerically evaluated variance of the walker's position as a function of time with initial state $|0\rangle (|+\rangle + i|-\rangle)/\sqrt{2}$: unitary evolution (blue solid), driven coin with $\kappa(t) = \cos(t/10)$ (red dot), and random walk (black solid). The walker's position distribution at (b) $t = 22$, (c) $t = 32$, (d) $t = 48$.

respectively.

If the coin state is initially $(|+\rangle + i|-\rangle)/\sqrt{2}$ and $P_w(x, 0) = \delta_{x0}$, then $P_w(x, t) = P_w(-x, t)$. The walker's spread is $\sigma(t) := \sqrt{V(t)}$ for $V = \langle x^2 \rangle - \langle x \rangle^2$ and $\langle x^m \rangle(t)$ the m^{th} moment of $P_w(x, t)$. Rate of spreading $\sigma(t)$ is widely used to differentiate between quantum and classical random walks. In diffusive transport, $V \propto t$, whereas $V \propto t^2$ for ballistic transport (which holds for the coherent quantum walk). For the random walk in the classical or quantum limit at long times, V 's growth is either diffusive or ballistic with no other spreading rate allowed [22, 23].

Driving the coin (5) with periodic $\kappa(t)$ affects the variance V as shown in Fig 1(a): V oscillates between classical diffusive and quantum ballistic values at various times t with an η -dependent period. Variances of the undriven-coin quantum walk and the classical random walk provide tight upper and lower bounds for the driven-coin time-dependent variance. Figures 1(b-d) display numerical results for the position distribution as a blend of classical and quantum distributions ($t = 22$), nearly fully quantum ($t = 32$) and nearly fully classical ($t = 48$).

The walker's evolution is often easier to analyze in the Fourier domain using ‘momentum’ states ($\hbar \equiv 1$)

$$|k\rangle = \sum_{x=-\infty}^{\infty} e^{ikx} |x\rangle, S|k\rangle = e^{-ik} |k\rangle, k \in \mathbb{R} \quad (8)$$

in whose basis the evolution is given by

$$U|k\rangle_w \otimes |\pm\rangle_c = |k\rangle \otimes H(k) |\Phi\rangle_c, H(k) = \frac{1}{2} \begin{pmatrix} e^{-ik} & e^{-ik} \\ e^{ik} & -e^{ik} \end{pmatrix}.$$

If the initial walker-coin state corresponds to the walker localized at the origin $x = 0$ and the coin in any pure

state $|\Phi\rangle_c$, the inverse transform expression

$$|x\rangle = \int_{-\pi}^{\pi} \frac{dk}{2\pi} e^{-ikx} |k\rangle. \quad (9)$$

yields the t -dependent joint walker-coin state

$$\rho(t) = \frac{1}{(2\pi)^2} \int_{-\pi}^{\pi} dk \int_{-\pi}^{\pi} dk' |k\rangle \langle k'| \otimes H^t(k) \rho_c (H^\dagger(k))^t. \quad (10)$$

After t steps the state is

$$\rho_{\text{wc}}(t) = \int_{-\pi}^{\pi} \frac{dk}{2\pi} \int_{-\pi}^{\pi} \frac{dk'}{2\pi} |k\rangle \langle k'| \otimes \mathcal{L}^t(k, k') \rho_c \quad (11)$$

for

$$\mathcal{L}(k, k') \hat{O} := \sum_{i \in \{0, \pm\}} H(k) A_i \hat{O} A_i^\dagger H^\dagger(k'). \quad (12)$$

For $k = k'$ this superoperator satisfies $\text{Tr}[\mathcal{L}^t(k, k') \hat{O}] = \text{Tr}[\hat{O}]$ for any \hat{O} so $\mathcal{L}(k, k')$ is trace-preserving.

Figure 1 is derived numerically hence not conclusive in revealing asymptotic spreading behavior arising from the periodically driven coin. Therefore, we exploit the momentum representation to derive the asymptotic long-time position distribution

$$P_w(x; t) = \int_{-\pi}^{\pi} \frac{dk}{2\pi} \int_{-\pi}^{\pi} \frac{dk'}{2\pi} e^{-i(k-k')x} \text{Tr} [\mathcal{L}^t(k, k') \rho_c] \quad (13)$$

of the driven-coin quantum walker. Using

$$\sum_{x=-\infty}^{\infty} x^m e^{-ix(k-k')} = 2\pi(-i)^m \delta^{(m)}(k - k'), \quad (14)$$

we obtain

$$\langle \hat{x}^m \rangle = (-1)^m \int_{-\pi}^{\pi} \frac{dk}{2\pi} \int_{-\pi}^{\pi} \frac{dk'}{2\pi} \delta^{(m)}(k - k') \text{Tr} \{ \mathcal{L}^t(k, k') \rho_c \}$$

so the first two moments are

$$\langle \hat{x} \rangle = - \int_{-\pi}^{\pi} \frac{dk}{2\pi} \sum_{j=1}^t \text{Tr} \{ Z \mathcal{L}^j(k, k) \rho_c \}. \quad (15)$$

and

$$\begin{aligned} \langle \hat{x}^2 \rangle = & - \int_{-\pi}^{\pi} \frac{dk}{2\pi} \left(\sum_{j=1}^t \sum_{j'=1}^j \text{Tr} \{ Z \mathcal{L}^{j-j'}(k, k) Z \mathcal{L}^{j'}(k, k) \rho_c \} \right. \\ & \left. + \sum_{j=1}^t \sum_{j'=1}^{j-1} \text{Tr} \{ Z \mathcal{L}^{j-j'}(k, k) \mathcal{L}^{j'}(k, k) \rho_c Z \} \right) \end{aligned} \quad (16)$$

with $Z = \begin{pmatrix} 1 & 0 \\ 0 & -1 \end{pmatrix}$. As $\mathcal{L}(k, k)$ is additive, we obtain

$$\begin{aligned} \mathcal{L}(k, k) \mathcal{E} \rho_c = & \kappa(t) \mathcal{L}(k, k) \rho_c \\ & + [1 - \kappa(t)] \mathcal{L}(k, k) [\mathcal{P}^+ \rho_c \mathcal{P}^+ + \mathcal{P}^- \rho_c \mathcal{P}^-] \end{aligned} \quad (17)$$

with the first term on the right-hand side corresponding to a quantum-walk mapping (these terms are indicated by superscript Q) for a time-dependent coin and the second term corresponding to coherence-destroying measurements that transform the quantum walk into the random walk (these terms are indicated by a superscript R). Now we exploit linearity to find asymptotic solutions to the first and second term separately.

To study the first term on the right-hand side of (17), let us specialize for the moment on the unitary case $\mathcal{L}(k, k)\hat{O} = H(k)\hat{O}H^\dagger(k)$, for which we employ representations of the pure walker-coin state $|\Phi\rangle_c = \sum c_l(k)|\phi_l(k)\rangle$ in terms of the orthogonal eigenvectors $|\phi_l(k)\rangle$ and corresponding eigenvalues $e^{i\theta_l(k)}$ of $H(k)$ for $k \in \mathbb{Z}$ and $l \in \{0, 1\}$. Note that $\theta_0(k) + \theta_1(k) = \pi$.

For the standard quantum walk with a Hadamard coin,

$$|\phi_l(k)\rangle = \sqrt{1 + \cos^2 k - (-1)^l \cos k} \sqrt{1 + \cos^2 k} \\ \times \left(\begin{array}{c} e^{-ik}/\sqrt{2} \\ e^{-i\theta_l(k)} - e^{-ik}/\sqrt{2} \end{array} \right). \quad (18)$$

The coin state

$$\rho_c(t) = H^t(k)|\Phi\rangle_c\langle\Phi|(H^\dagger(k))^t \\ = \sum_{l,l'} c_l^*(k)c_{l'}(k)|\phi_{l'}(k)\rangle\langle\phi_l(k)|e^{i[\theta_{l'}(k)-\theta_l(k)]t}$$

after t steps is substituted into Eqs. (15) and (16) to yield

$$\langle\hat{x}\rangle^Q = t - \int \frac{dk}{\pi} \sum_{l,l'} c_l^*(k)c_{l'}(k) \mathcal{P}_{ll'}^+(k) \sum_{j=1}^t e^{ij[\theta_{l'}(k)-\theta_l(k)]}, \\ \langle\hat{x}^2\rangle^Q = \int \frac{dk}{2\pi} \sum_{l,l',l''} c_l^*(k)c_{l'}(k) Z_{ll'}(k) Z_{l'l''}(k) \\ \times \sum_{j,j'=1}^t e^{ij[\theta_{l'}(k)-\theta_l(k)]} e^{ij'[\theta_{l'}(k)-\theta_{l''}(k)]},$$

$$\mathcal{P}_{ll'}^+(k) = \langle\phi_l(k)|\mathcal{P}^+|\phi_{l'}(k)\rangle, Z_{ll'}(k) = \langle\phi_l(k)|Z|\phi_{l'}(k)\rangle.$$

As $H(k)$ is nondegenerate and θ_{k0} and θ_{k1} are distinct, most terms for $\langle\hat{x}\rangle^Q$ and $\langle\hat{x}^2\rangle^Q$ above oscillate strongly, and only diagonal ($k = k'$) terms survive in the long-time limit. Inserting Eq. (18) into the equations above yields

$$V^Q \xrightarrow{t \rightarrow \infty} t^2(C_2 - C_1^2), \quad (19)$$

$$C_1 = 1 - \int_{-\pi}^{\pi} \frac{dk}{\pi} \sum_{l=1,2} |c_l(k)|^2 P_{ll}^+(k) \\ = 1 - \int_{-\pi}^{\pi} \frac{dk}{2\pi(1+\cos^2 k)} = 1 - \frac{1}{\sqrt{2}}, \\ C_2 = 1 - \int_{-\pi}^{\pi} \frac{dk}{\pi} 2 \sum_{l=1,2} |c_l(k)|^2 P_{ll}^+(k) P_{ll}^-(k) \\ = 1 - \int_{-\pi}^{\pi} \frac{dk}{2\pi(1+\cos^2 k)} = 1 - \frac{1}{\sqrt{2}}. \quad (20)$$

By path integration [24],

$$P_w^Q(x,t) \approx \left(\frac{1}{2\pi}\right)^2 \int_{-\pi}^{\pi} dk \int_{-\pi}^{\pi} \pi dk' e^{-ix(k-k')} \\ \times \sum_{l,l'} c_l^*(k)c_{l'}(k') e^{-i[\theta_{l'}(k')-\theta_l(k)]t} \langle\phi_l(k)|\phi_{l'}(k')\rangle \\ \approx \int_{-\pi}^{\pi} dk \frac{1+(-1)^{x+t}}{\pi t \frac{\sin k}{(1+\cos^2 k)^{3/2}}} \left\{ \left(1 - \frac{x}{t}\right)^2 \right. \\ \times \cos^2 \left[\arcsin \left(\frac{\sin k}{\sqrt{2}} \right) t + xk - \frac{\pi}{4} \right] \\ + \left[1 - \left(\frac{x}{t} \right)^2 \right] \cos^2 \left[\arcsin \left(\frac{\sin k}{\sqrt{2}} \right) t \right. \\ \left. \left. + (x-1)k - \frac{\pi}{4} \right] \right\},$$

which agrees well with the non-asymptotic numerical results shown in Fig. 2.

Now we proceed to study the second (random-walk) term of Eq. (17). From Eq. (11), the representation $\hat{O} = r_1 \mathbb{1} + r_2 X + r_3 Y + r_4 Z$ (Pauli representation) [19] yields

$$\mathcal{L}(k, k)\hat{O} = \begin{pmatrix} 1 & 0 & 0 & 0 \\ 0 & 0 & 0 & \cos 2k \\ 0 & 0 & 0 & -\sin 2k \\ 0 & 0 & 0 & 0 \end{pmatrix} \begin{pmatrix} r_1 \\ r_2 \\ r_3 \\ r_4 \end{pmatrix}, \quad (21)$$

which leads to new expressions for the first two moments

$$\langle\hat{x}\rangle^R = - \int_{-\pi}^{\pi} \frac{dk}{2\pi} (0 \ 0 \ 0 \ 1) \left(\sum_{j=1}^t \mathcal{L}^j(k, k) \right) \begin{pmatrix} r_1 \\ r_2 \\ r_3 \\ r_4 \end{pmatrix} = 0, \\ \langle\hat{x}^2\rangle^R = t - \int_{-\pi}^{\pi} \frac{dk}{2\pi} (1 \ 0 \ 0 \ 0) \left[Z_L \sum_{j=1}^t \sum_{j'=1}^{j-1} \mathcal{L}^{j-j'}(k, k) \right. \\ \times (Z_L + Z_R) \mathcal{L}^{j'}(k, k) \left. \begin{pmatrix} r_1 \\ r_2 \\ r_3 \\ r_4 \end{pmatrix} \right] = t, \quad (22)$$

$$Z_L = \begin{pmatrix} 0 & 0 & 0 & 1 \\ 0 & 0 & i & 0 \\ 0 & -i & 0 & 0 \\ 1 & 0 & 0 & 0 \end{pmatrix}, Z_R = \begin{pmatrix} 0 & 0 & 0 & 1 \\ 0 & 0 & -i & 0 \\ 0 & i & 0 & 0 \\ 1 & 0 & 0 & 0 \end{pmatrix}. \quad (23)$$

As $\langle\hat{x}\rangle^R = 0$, $\langle\hat{x}^2\rangle^R$ equals the variance and is purely diffusive as is evident from its proportionality with t . The asymptotic binomial random-walk position distribution evaluated only over even (odd) x for even (odd) t is thus

$$P_w^R(x, t) = \frac{1}{2^t} \frac{t!}{\left[\frac{t-x}{2}\right]! \left[\frac{t+x}{2}\right]!}. \quad (24)$$

Thus, for a QW with a driven coin, we have the asymptotic position distribution

$$P_w(x, t) = \kappa P_w^Q(x, t) + (1 - \kappa) P_w^R(x, t) \quad (25)$$

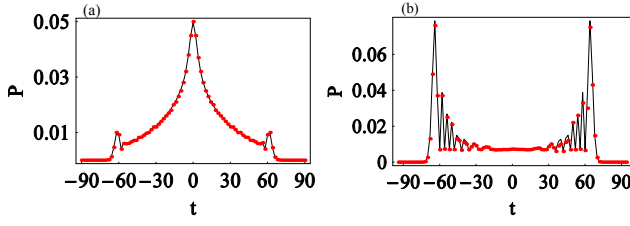


FIG. 2: (Color online) Walker position distributions $P(x, t)$ for even values of x and (a) $t = 90$ and (b) $t = 94$ with initial state $|0\rangle (|+\rangle + i|-\rangle)/\sqrt{2}$ and driven-coin function $\kappa(t) = \cos(t/10)$ for precise numerical simulations (dots) and asymptotic expression (solid).

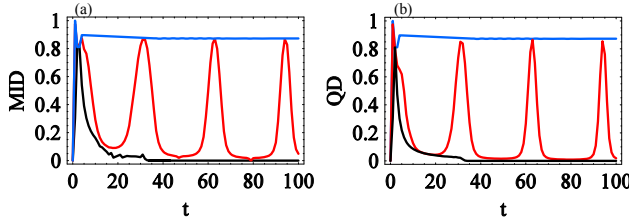


FIG. 3: (Color online) (a) The MID and (b) QD for a QW on a line after $t = 100$ steps for undriven (blue), driven with $\kappa(t) = \cos(t/10)$ (red) and random walk (black) cases with initial state $|0\rangle (|+\rangle + i|-\rangle)/\sqrt{2}$.

and variance

$$V = \kappa V^Q + (1 - \kappa)t. \quad (26)$$

Excellent agreement between analytical asymptotic expressions and numerical results in the long-time limit is observed, for example in the walker's position distribution as shown in Fig. 2.

Although the usual signature of the quantum walk is the rate of spreading (26), which, for the driven coin, is a weighted sum of the quantum ballistic spread V^Q and the diffusive term V^R proportional to t , the quantum-classical divide can be explored in more depth through studying entanglement between the walker and the coin. Entanglement should be zero in the random-walk case and should generally be non-zero in the quantum-walk case. We analyze quantum correlation between the walker and the driven coin using two measures: measurement induced disturbance (MID) [25] and quantum discord (QD) [26].

Ollivier and Zurek [26] made use of von Neumann-type measurements to quantify QD, which consist of one-dimensional projectors summing to the identity operator. Here we introduce the projection operators $\{B_j\}$ to describe a von Neumann-type measurement for coin state only. The quantum conditional entropy with respect to this measurement is given by

$$S[\rho_{wc}(t)|\{B_j\}] := \sum_j p_j S[\rho_j(t)], \quad (27)$$

and the associated quantum mutual information of this measurement is defined as

$$\mathcal{I}[\rho_{wc}(t)|\{B_j\}] := S[\rho_w(t)] - S[\rho_{wc}(t)|\{B_j\}], \quad (28)$$

where the conditional density operator operator

$$\rho_j(t) = (\mathbb{1} \otimes B_j)\rho_{wc}(t)(\mathbb{1} \otimes B_j) \quad (29)$$

with the measurement result j , and the probability

$$p_j = \text{Tr}[(\mathbb{1} \otimes B_j)\rho_{wc}(t)(\mathbb{1} \otimes B_j)]. \quad (30)$$

The classical correlations are

$$\mathcal{C}_c[\rho_{wc}(t)] := \sup_{B_j} \mathcal{I}[\rho_{wc}(t)|\{B_j\}]. \quad (31)$$

QD is characterized as

$$D := \mathcal{I}[\rho_{wc}(t)] - \mathcal{C}_c[\rho_{wc}(t)] \quad (32)$$

and quantifies genuine quantum correlation between the walker and coin. With respect to QD, correlations between ρ_w and ρ_c are classical if there exists a unique local measurement strategy on the coin $\{B_j\}$ leaving $\rho_i(t)$ unaltered from the original joint walker-coin state $\rho_{wc}(t)$. Calculating QD is difficult due to the need to maximize over all possible von Neumann-type measurements of the coin state in order to determine the classical correlation.

MID has an advantage over QD in that MID is operational but tends to overestimate non-classicality because of a lack of optimization over local measurements. We therefore ascertain whether the joint walker-coin state is 'quantum' by determining if a local measurement strategy exists that leaves the state unchanged. The MID is [25]

$$Q[\rho_{wc}(t)] := \mathcal{I}[\rho_{wc}(t)] - \mathcal{I}[\rho_{wc}(t)|\{B_j\}] \quad (33)$$

which is the difference between the quantum and classical mutual information.

We numerically evaluate MID and QD for a QW in the undriven, driven-coin and random-walk cases and display results in Fig. 3. These quantities reveal the degree of quantum correlation between the walker and the coin. For the undriven-coin case, MID and QD are the same. For the driven-coin case, MID and QD exhibit quantum-correlation oscillations with the same period as for the position-variance oscillation. Thus, the interpretation of diffusive and ballistic spreading as classical and quantum features is sound, but the quantum-to-classical transition is indeed reversible as observed in the quantum-correlation plots.

In summary we study the driven-coin quantum walk and show that position spreading is an appropriate signature of classical vs quantum behavior and that controlling the driven coin can control the quantum-to-classical transition and even reverse this transition. Our results are determined by numerical means for all times and by

closed-form expressions in the asymptotically long-time limit. We have proven that the walker's reduced position distribution is an incoherent mixture (sum) of classical- and quantum-walk distributions. The periodically-driven coin case provides a clear illustration of this reversible quantum-to-classical transition, but our results are valid for general driven-coin cases. We show that the reversible quantum-to-classical transition is manifested even at the level of walker-coin quantum correlations. Our 'reversible decoherence' results could be valuable for tuning quantum walks [21] and especially challenge notions of decoherence in quantum walks by showing reversibility.

PX acknowledges financial support from NSFC and China's 973 Program, and BCS acknowledges financial support from CIFAR, NSERC and AITF.

-
- [1] J. Kempe, *Cont. Phys.* **44**, 307 (2003), to appear, quant-ph/0303081.
- [2] J. Kempe, in *Proc. 7th Intl. Workshop on Randomization and Approximation Techniques in Computer Science (RANDOM '03)* (2003), to appear, quant-ph/0205083.
- [3] V. Kendon, *Where to quantum walk*, arXiv:1107.3795 (2011).
- [4] M. Santha, in *TAMC* (2008), pp. 31–46.
- [5] A. M. Childs, R. Cleve, E. Deotto, E. Farhi, S. Gutmann, and D. A. Spielman, in *Proc. 35th Annual ACM Symposium on Theory of Computing (STOC'03)* (ACM, New York, 2003), pp. 59–68, quant-ph/0209131.
- [6] N. Shenvi, J. Kempe, and K. B. Whaley, *Phys. Rev. A* **67**, 052307 (2003), URL <http://link.aps.org/doi/10.1103/PhysRevA.67.052307>.
- [7] A. Kay, *International Journal of Quantum Information* **08**, 641 (2010), URL <http://www.worldscientific.com/doi/abs/10.1142/S0219749910006514>.
- [8] M. Mohseni, P. Rebentrost, S. Lloyd, and A. Aspuru-Guzik, *The Journal of Chemical Physics* **129**, 174106 (pages 9) (2008), URL <http://link.aip.org/link/?JCP/129/174106/1>.
- [9] A. M. Childs, *Phys. Rev. Lett.* **102**, 180501 (2009), URL <http://link.aps.org/doi/10.1103/PhysRevLett.102.180501>.
- [10] A. M. Childs, D. Gosset, and Z. Webb, *Universal quantum computation by multi-particle quantum walks*, arXiv:1205.3782 (2012).
- [11] D. Deutsch, *Proc. Roy. Soc. Lond. A* **400**, 97 (1985).
- [12] R. Raussendorf and H. J. Briegel, *Phys. Rev. Lett.* **86**, 5188 (2001), URL <http://link.aps.org/doi/10.1103/PhysRevLett.86.5188>.
- [13] E. Farhi, J. Goldstone, S. Gutmann, J. Lapan, A. Lundgren, and D. Preda, *Science* **292**, 472 (2001).
- [14] C. Nayak, S. H. Simon, A. Stern, M. Freedman, and S. Das Sarma, *Rev. Mod. Phys.* **80**, 1083 (2008), URL <http://link.aps.org/doi/10.1103/RevModPhys.80.1083>.
- [15] C. A. Ryan, M. Laforest, J. C. Boileau, and R. Laflamme, *Phys. Rev. A* **72**, 062317 (2005), URL <http://link.aps.org/doi/10.1103/PhysRevA.72.062317>.
- [16] F. Zähringer, G. Kirchmair, R. Gerritsma, E. Solano, R. Blatt, and C. F. Roos, *Phys. Rev. Lett.* **104**, 100503 (2010), URL <http://link.aps.org/doi/10.1103/PhysRevLett.104.100503>.
- [17] M. A. Broome, A. Fedrizzi, B. P. Lanyon, I. Kassal, A. Aspuru-Guzik, and A. G. White, *Phys. Rev. Lett.* **104**, 153602 (2010), URL <http://link.aps.org/doi/10.1103/PhysRevLett.104.153602>.
- [18] A. Schreiber, K. N. Cassemiro, V. Potoček, A. Gábris, I. Jex, and C. Silberhorn, *Phys. Rev. Lett.* **106**, 180403 (2011), URL <http://link.aps.org/doi/10.1103/PhysRevLett.106.180403>.
- [19] T. A. Brun, H. A. Carteret, and A. Ambainis, *Phys. Rev. Lett.* **91**, 130602 (2003), URL <http://link.aps.org/doi/10.1103/PhysRevLett.91.130602>.
- [20] T. A. Brun, H. A. Carteret, and A. Ambainis, *Phys. Rev. A* **67**, 032304 (2003), URL <http://link.aps.org/doi/10.1103/PhysRevA.67.032304>.
- [21] V. Kendon, *Mathematical Structures in Comp. Sci.* **17**, 1169 (2007), ISSN 0960-1295, URL <http://dx.doi.org/10.1017/S0960129507006354>.
- [22] A. Ahlbrecht, H. Vogts, A. H. Werner, and R. F. Werner, *J. Math. Phys.* **52**, 042201 (2011).
- [23] A. Ahlbrecht, A. Alberti, D. Meschede, V. B. Scholz, A. H. Werner, and R. F. Werner, *New J. Phys.* (2012).
[24] A. Ahlbrecht and A. Vishwanath, *Quantum walk on the line*, arXiv:quant-ph/0010117 (2000).
- [25] S. Luo, *Phys. Rev. A* **77**, 022301 (2008), URL <http://link.aps.org/doi/10.1103/PhysRevA.77.022301>.
- [26] H. Ollivier and W. H. Zurek, *Phys. Rev. Lett.* **88**, 017901 (2001), URL <http://link.aps.org/doi/10.1103/PhysRevLett.88.017901>.